Electronic Supplementary Material (ESI) for Energy .

# Supporting Information for

## A long-life lithium-ion battery with highly porous $TiNb_2O_7$ anode for large-scale electrical energy storage

**Authors:** Bingkun Guo[1†*], Xiqian Yu[2†], Xiao-Guang Sun[1], Miaofang Chi[3], Zhen-An Qiao[1], Jue Liu[2], Yong-Sheng Hu[4*], Xiao-Qing Yang[2], John B. Goodenough[5], Sheng Dai[1, 6*]

**Affiliations:**

[1]Chemical Sciences Division, Oak Ridge National Laboratory, Oak Ridge, TN 37831(USA)

[2]Brookhaven National Laboratory, Upton, New York 11973 (USA).

[3]Center for Nanophase Materials Sciences, Oak Ridge National Laboratory, Oak Ridge, Tennessee (USA)

[4]Beijing National Laboratory for Condensed Matter Physics, Institute of Physics, Chinese Academy of Sciences, Beijing 100190 (China)

[5]Department of Mechanical Engineering, University of Texas at Austin, Austin, Texas 78712 (USA)

[6]Department of Chemistry, University of Tennessee, Knoxville, TN 37996 (USA)

*To whom correspondence should be addressed. E-mail: dais@ornl.gov, guobkun@hotmail.com, yshu@aphy.iphy.ac.cn.

### Experimental Section

### Methods

Nanoporous $TiNb_2O_7$ samples were synthesized using a sol-gel method. In a typical synthesis, 4.8 g F127 were dissolved in a mixture solution of 90 ml ethanol, 6 ml HCl and 7 ml HOAc. After stirring for 1 h, 20 mmol of niobium ethoxide ($Nb(OC_2H_5)_5$, Sigma-Aldrich) and 10 mmol tetrabutyl orthotitanate ($Ti(OC_4H_9)_4$, Sigma-Aldrich) were added into the solution. After stirring vigorously for 1 h, the mixture was transferred into a Petri dish and dried at 60 °C for 12 h. As-synthesized hybrids were calcined at different temperatures (600 °C, 700 °C, 850 °C, 1000 °C) in air for 3 h (ramp rate 10 $^{o}$C/min) to obtain $TiNb_2O_7$ samples (named as TNO-600, TNO-700, TNO-850 and TNO-1000, respectively).

$LiNi_{0.5}Mn_{1.5}O_4$ was prepared by a hydroxide precursor method[1, 2]. $Mn_{0.75}Ni_{0.25}(OH)_2$ was obtained via a coprecipitation method by drop-by-drop adding required amounts of the aqueous metal acetate solution (Mn:Ni=0.75:0.25) into a KOH solution under continuous stirring. The coprecipitated powder was washed with distilled water and dried in an oven at 100 $^{o}$C. As-synthesized $Mn_{0.75}Ni_{0.25}(OH)_2$ mixed with a required amount of LiOH and the mixture was calcined at 900 $^{o}$C in air for 12 h.

**Characterizations**

Nitrogen adsorption isotherms were measured at -196 ºC using TriStar 3000 volumetric adsorption analyzer manufactured by Micromeritics Instrument Corp. (Norcross, GA). Before adsorption measurements, the as-prepared samples were degassed in flowing nitrogen for 2 h at 200 ºC. The specific surface area of the samples was calculated using the Brunauer-Emmett-Teller (BET) method within the relative pressure range of 0.05 to 0.20. Pore size distribution plots were derived from the adsorption branch of the isotherms based on the BJH model. SEM images were recorded on a Hitachi HD-2000 SEM microscope operating at 200 kV. TEM was carried out on a FEI Titan 60/300 (S) TEM microscope equipped with a Gatan Image Filter (GIF) Quantum.

*In situ* XRD patterns were collected at beamline X14A of the National Synchrotron Light Source (NSLS) at Brookhaven national laboratory, with a linear position-sensitive silicon detector. The wavelength used was 0.77376 Å. *In situ* XAS experiments were performed at beamline X18A in transmission mode with a Si (111) double-crystal monochromator detuned to the 35-45% value of its original maximum intensity to eliminate the higher order harmonics. The reference spectrum of each element was simultaneously collected with the corresponding spectrum of the *in situ* cells by using a reference metal foil. Energy calibration was carried out with the first inflection point of the K-edge spectrum of the reference metal foil (i.e., Ti: 4966 eV). X-ray Absorption Near Edge Structure (XANES) and Extended X-ray Absorption Fine Structure (EXAFS) data were analyzed by the ATHENA software package.

Electrochemical experiments were carried out by using coin cells. The working electrode was prepared by mixing the as-synthesized materials, carbon black and poly(vinylidenedifluoride), PVDF at a weight ratio of 75:15:10. The slurry was casted onto Cu foil and dried under an infrared lamp to remove the solvent, followed by drying in a vacuum oven at 110 ºC for 12 h. The loading of active materials was 1.5-2.0 mg cm$^{-2}$. For the TNO- $LiNi_{0.5}Mn_{1.5}O_4$ full-cell, the anode is limited and the weight ratio of the cathode and the anode is 2.7:1. The capacity of full-cell was calculated based on the mass of the TNO electrode. Celgard 2320 used as separator and lithium foil was used as both counter and reference electrode. The electrolyte was consisted of a solution of 1 M $LiPF_6$ in ethylene carbonate (EC)/dimethyl carbonate (DMC)/diethyl carbonate (DEC) (1:1:1 by volume). The carbonates and $LiPF_6$ were obtained from Novolyte Corporation. The cells were assembled in an argon-filled glove box with moisture and oxygen level below 0.5 ppm. Galvanostatic discharge-charge experiments were tested in the voltage range of 1.0-3.0 V on an Arbin battery test system.

(1) J. Liu, A. Manthiram, *Chem Mater* **2009**, *21*, 1695.
(2) J. Liu, A. Manthiram, *J Electrochem Soc* **2009**, *156*, A66.

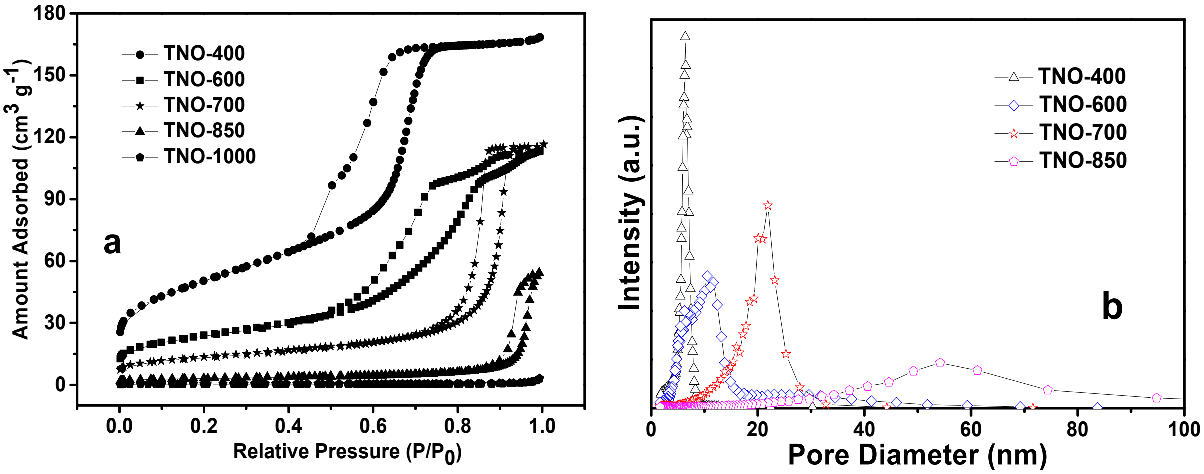

Figure S1 (a) Nitrogen adsorption-desorption isotherms and (b) corresponding pore size distribution curves for the Titanium-niobium oxides thermally treated at different temperatures (400 °C, 600 °C, 700 °C, 850 °C, 1000 °C).

Table S1 The BET Surface Area, Pore Size and Pore Volume for for the Titanium-niobium oxides thermally treated at different temperatures (400 °C, 600 °C, 700 °C, 850 °C).

| Samples | BET surface area (m$^2$ g$^{-1}$) | Pore size (nm) | Pore Volume (cm$^3$ g$^{-1}$) |
|---|---|---|---|
| TNO-400 | 182 | 5.6 | 0.26 |
| TNO-600 | 85 | 5.5-12 | 0.18 |
| TNO-700 | 48 | 22 | 0.15 |
| TNO-850 | 11 | 40-100 | 0.03 |

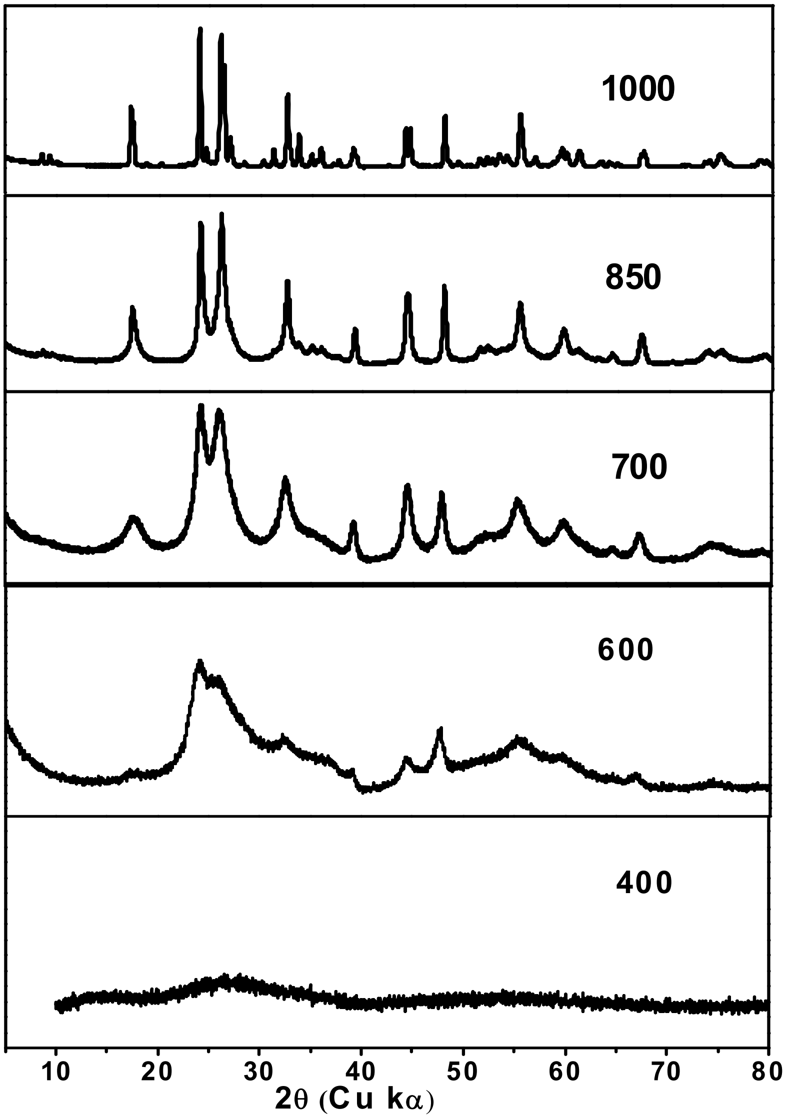

Figure S2. XRD patterns of the samples synthesized at 400°C, 600°C, 700°C, 850°C and 1000°C.

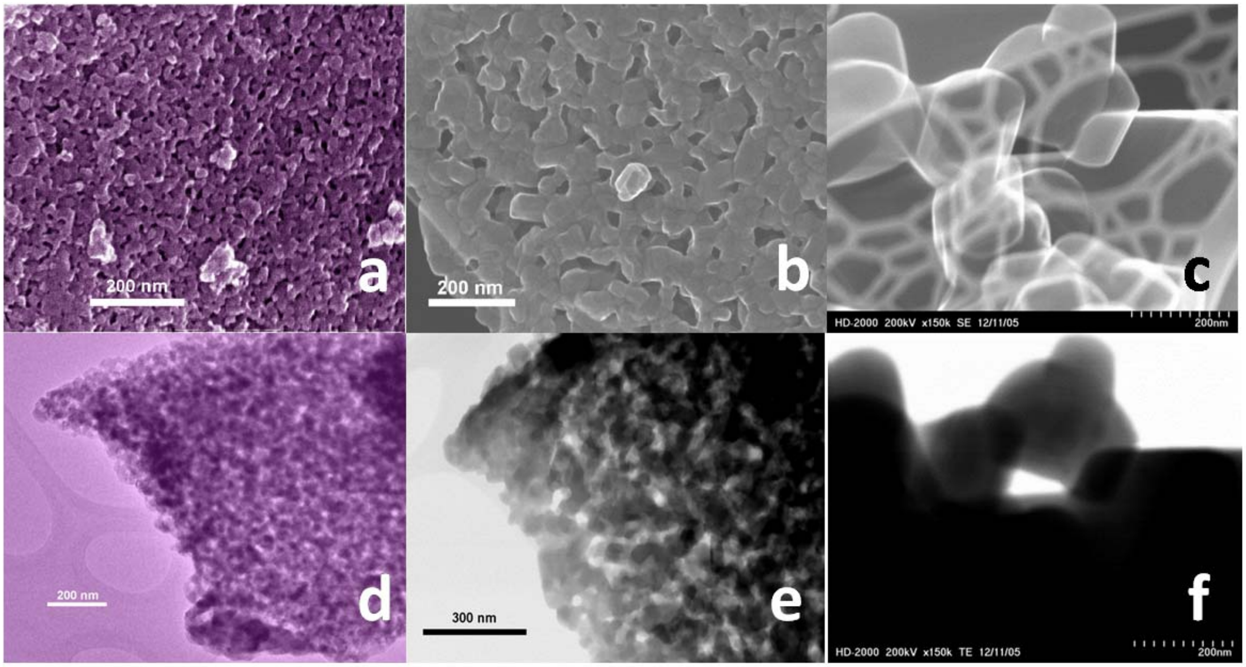

Figure S3 SEM images of TNO-700 (a), TNO-850 (b) and TNO-1000 (c); TEM images of TNO-700 (d), TNO-850 (e) and TNO-1000 (f).

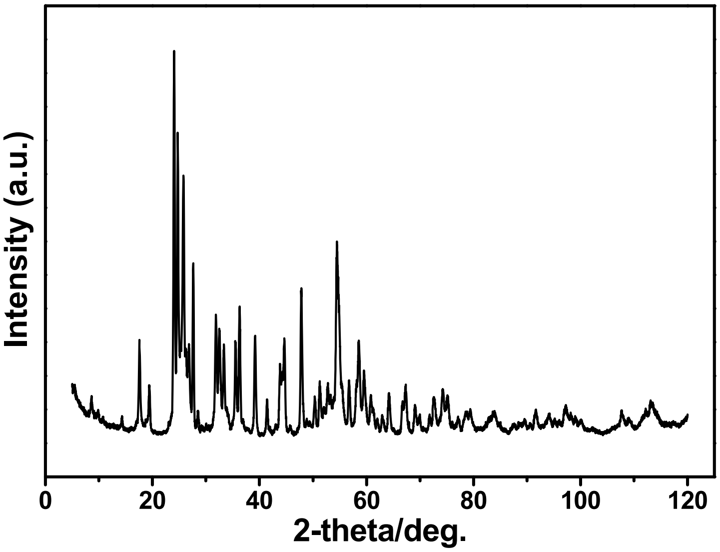

Figure S4 XRD pattern of the $TiNb_2O_7$-Solid-State-1000 sample. (Some impurity phases can still be observed even after treated at 1000 $^{o}$C for 3 h for the sample sythesized by a solid-state approach.)

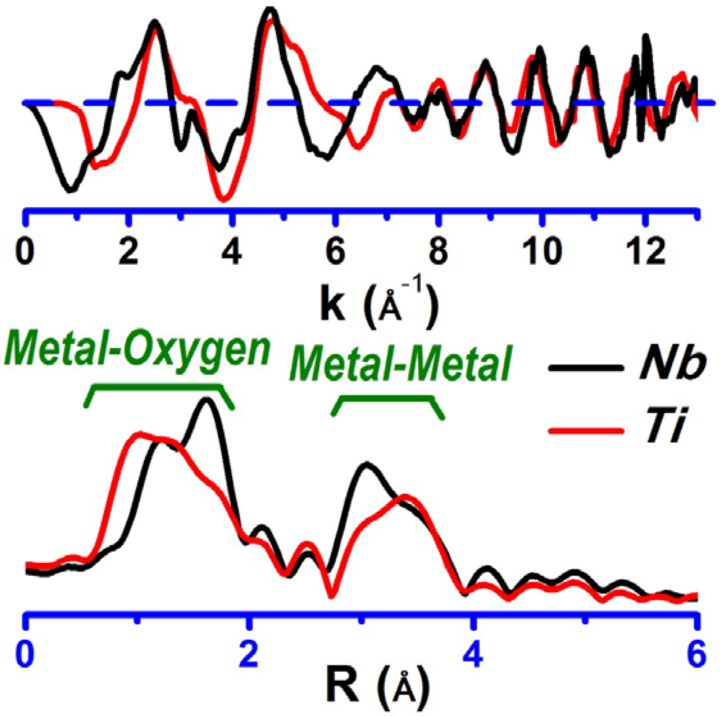

Figure S5 $k^2$-weighted Ti and Nb K-edge EXAFS spectra and corresponding $k^2$-weighted Fourier transforms of $TiNb_2O_7$ (700°C sample).

X-ray absorption spectroscopy (XAS) experiments were further performed to investigate the local environment around Ti and Nb sites in the pristine material. The $k^2$-weighted $\chi(k)$ and the corresponding Fourier transformed (FT) EXAFS are shown in Figure S6. They are both similar in appearance within the whole observation region, which is indicative of similar local environment around Ti and Nb in the $TiNb_2O_7$ structure. A slight difference of the EXAFS between Ti and Nb may be ascribed to the edge and corner site preference of the $Ti^{4+}$. These results suggest an almost random Ti/Nb occupancy at each atomic site. Clearly, titanium-niobium oxides with interconnected nanoporous framework composed of nanocrystals were successfully prepared by a facile approach.

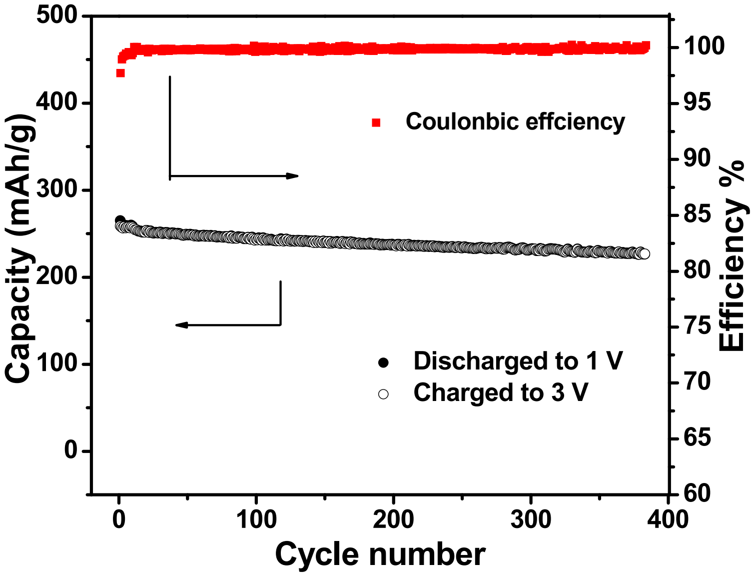

Figure S6 Cyclic performance of the nanoporous TNO-700 sample at a current rate of 1C (387 mA $g^{-1}$).

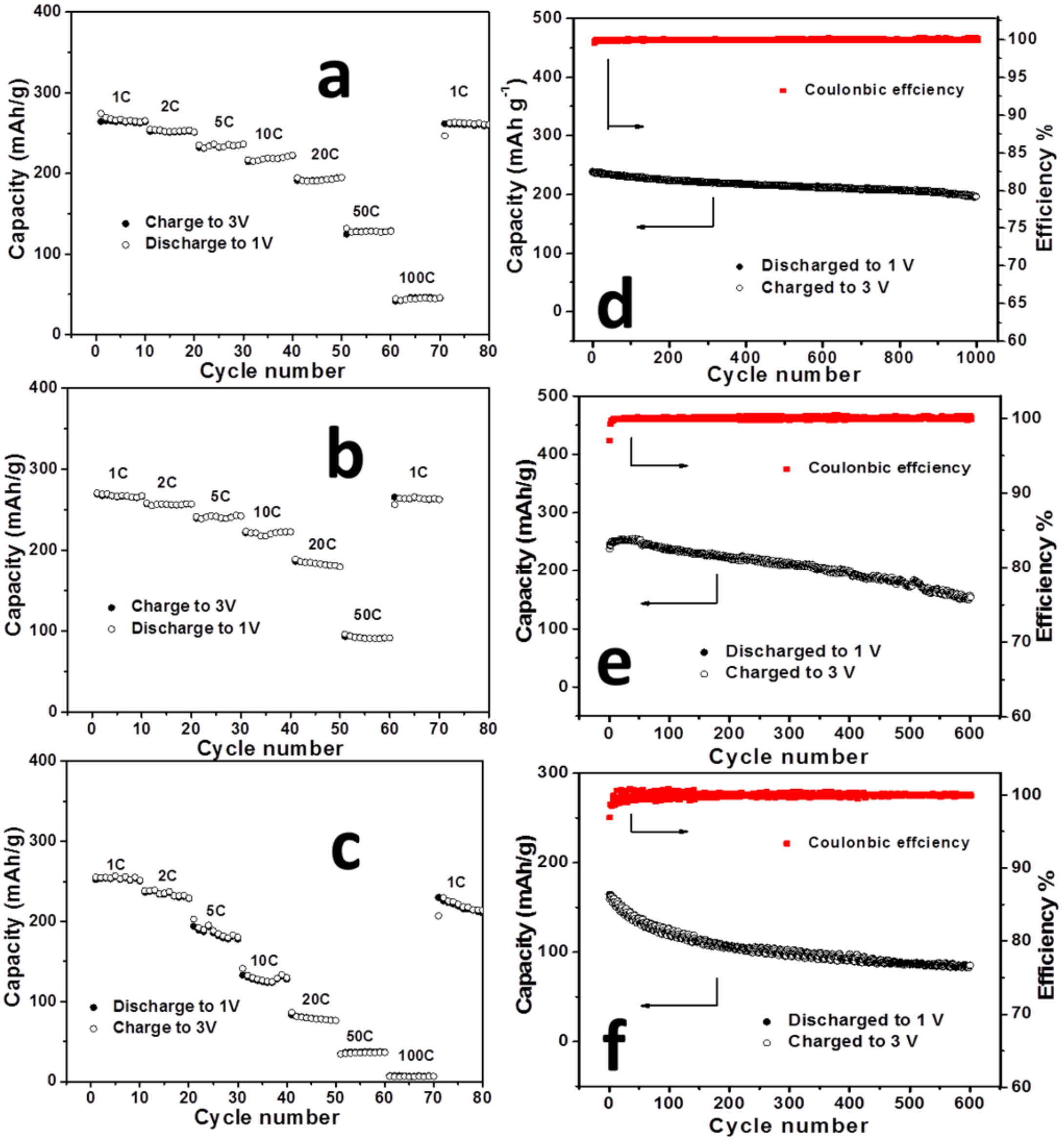

Figure S7 Rate performance of the TNO-700 (a), TNO-850(b) and TNO-1000 (c); Cyclic performance of the TNO-700 (d), TNO-850 (e) and TNO-1000 (f) at a current rate of 5C after aging at 0.1C for 5 cycles.

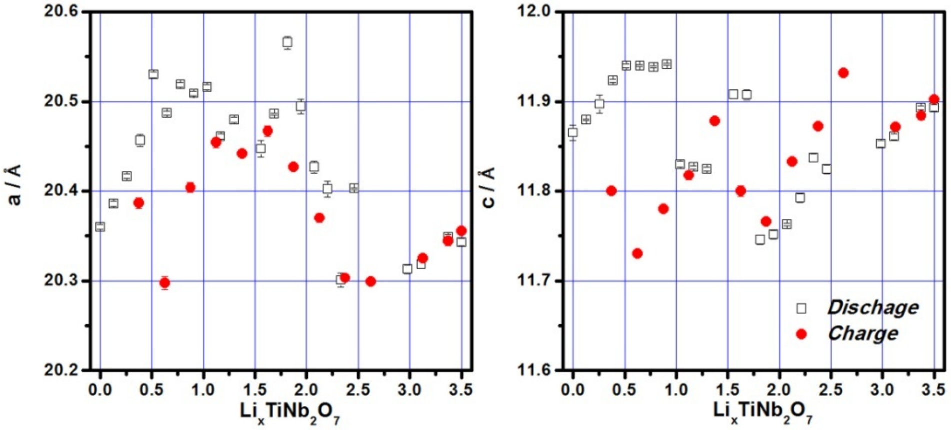

Figure S8 Lattice constant *a* and *c* vs. *x* calculated from Label fitting of $Li_xTiNb_2O_7$ (open circle: during discharge; solid dot: during charge)

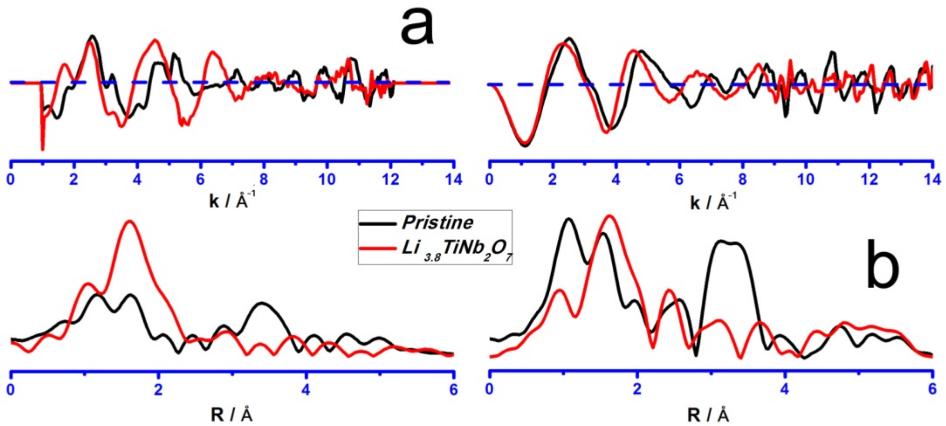

Figure S9 k$^2$-weighted EXAFS spectra and corresponding k$^2$-weighted Fourier transforms of (a) Ti and (b) Nb at the pristine and discharged states (0.8 V, $Li_{3.8}TiNb_2O_7$)

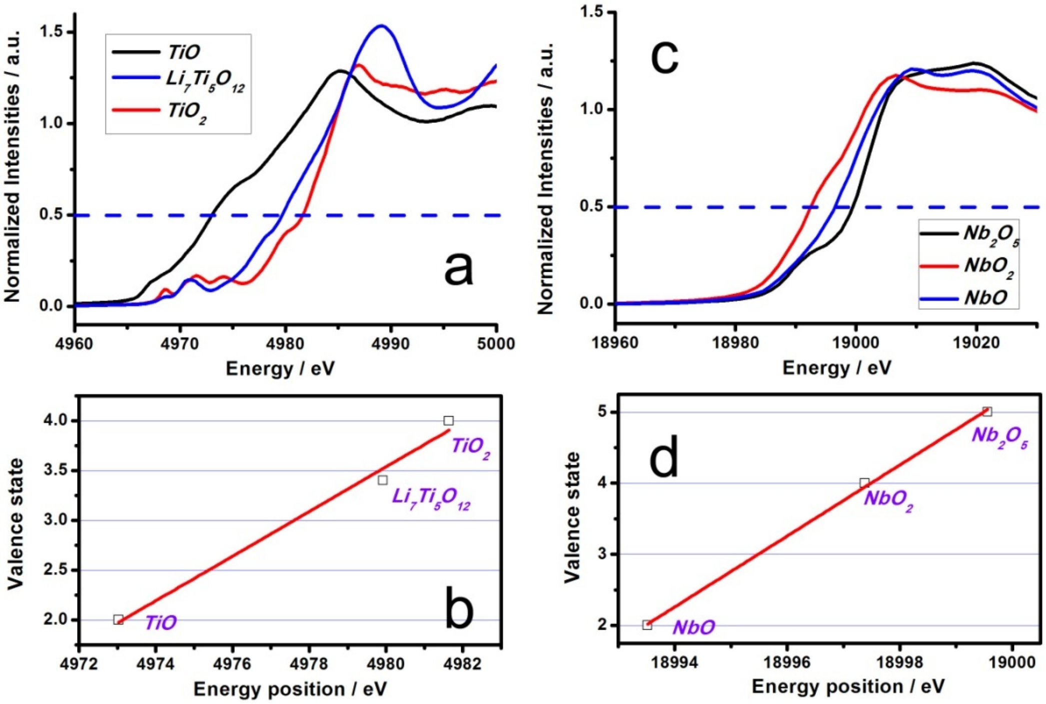

Figure S10 K-edge XANES spectra of reference standard materials of (a) Ti and (c) Nb and their valance state relationship with edge energy position (b) Ti and (d) Nb .

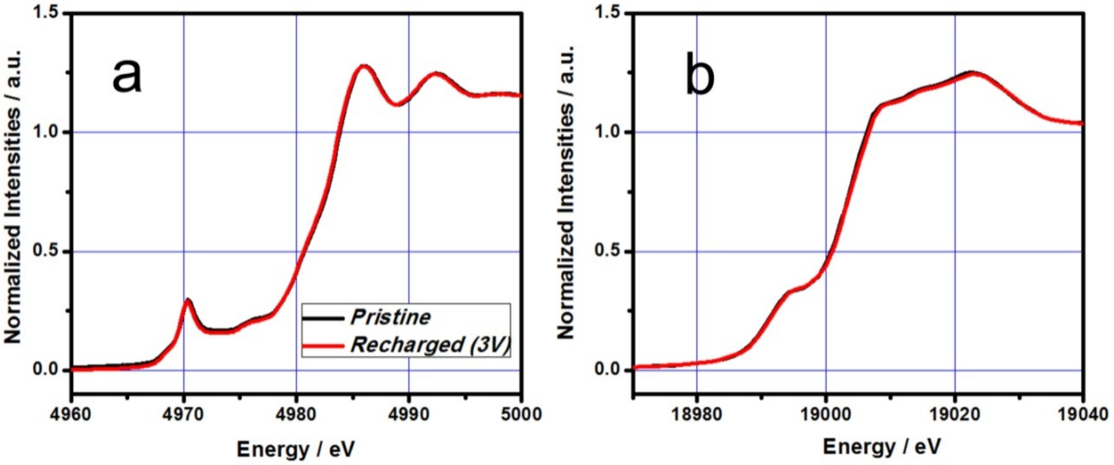

Figure S11 Comparison of XANES spectra of (a) Ti and (b) Nb at the pristine and recharged states (3.0 V)

The apparent chemical diffusion coefficient was calculated from the Randles–Sevcik equation:

$$I_p = 0.4463n^{3/2}F^{3/2}CSR^{-1/2}T^{-1/2}D_{Li}^{1/2}v^{1/2} \quad (1)$$

where $I_p$ is the peak current (A), n is the charge transfer number, F is the Faraday's constant (96486 C $mol^{-1}$), C is the concentration, S is the surface area of the electrode ($cm^2$), R is the gas constant (8.314 J $mol^{-1}$ $K^{-1}$), T is the absolute temperature (K), $D_{Li}$ the chemical diffusion coefficient ($cm^2$ $s^{-1}$) measured by CV, and $v$ is the scanning rate (V $s^{-1}$).

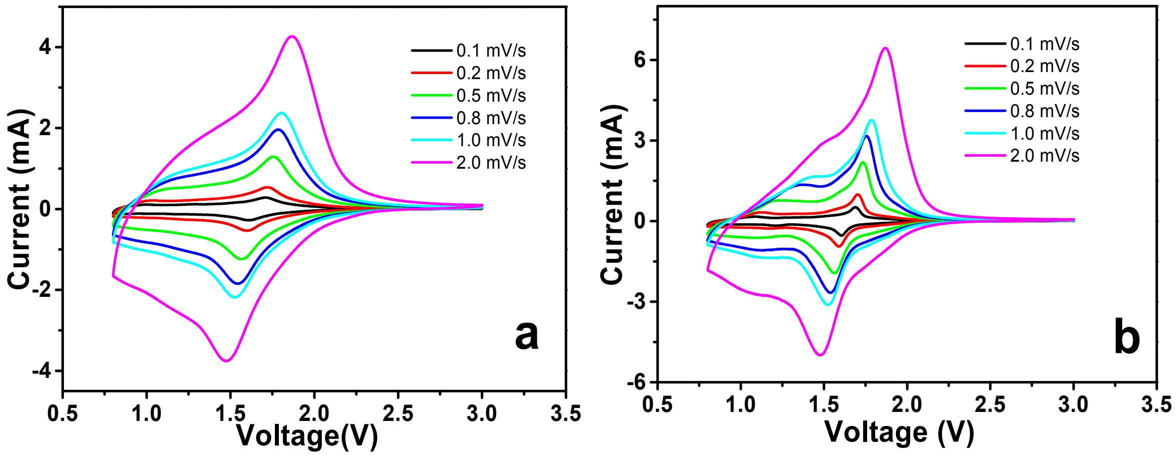

Figure S12 Cyclic Voltammograms of the TNO-700 (a) and TNO-850 (b) for various sweep rates.

Table S2 The apparent chemical diffusion coefficient of lithium ($D_{Li}$) in TNO-700 and TNO-850 samples based on the cyclic voltammetry experiments.

| $D_{Li}$ | TNO-700 | TNO-850 |
|---|---|---|
| Lithiation ($cm^2/s$) | $2.0\times10^{-12}$ | $1.8\times10^{-12}$ |
| Delithiation ($cm^2/s$) | $3.0\times10^{-12}$ | $2.7\times10^{-12}$ |

The lower $D_{Li}$ value in the lithiation process than that in the delithiation process is consistent with the rate test showing that the discharge process (Li-insertion) is the rate-limiting step.